Geophysical Research Letters

RESEARCH LETTER
10.1029/2022GL098242

Reconstruction of Violent Tornado Environments in Europe: High-Resolution Dynamical Downscaling of ERA5

Natalia Pilguj[1], Mateusz Taszarek[2,3], Maciej Kryza[1], and Harold E. Brooks[2,4]

[1]Faculty of Earth Sciences and Environmental Management, University of Wrocław, Wrocław, Poland, [2]National Severe Storms Laboratory, Norman, OK, USA, [3]Department of Meteorology and Climatology, Adam Mickiewicz University, Poznań, Poland, [4]School of Meteorology, University of Oklahoma, Norman, OK, USA

Key Points:

- Tornadoes were accompanied by a mean 0–6 km wind shear of 24.3 m s^{-1} and mean convective available potential energy of 1678 J kg^{-1}
- Dynamical downscaling with WRF model indicated more favorable near-ground wind profile compared to initial ERA5 conditions
- In 8 out of 12 violent tornado events, the WRF model simulated updraft helicity tracks in the area of a favorable tornado environment

Supporting Information:

Supporting Information may be found in the online version of this article.

Correspondence to:

N. Pilguj,
natalia.pilguj@uwr.edu.pl

Citation:

Pilguj, N., Taszarek, M., Kryza, M., & Brooks, H. (2022). Reconstruction of violent tornado environments in Europe: High-resolution dynamical downscaling of ERA5. *Geophysical Research Letters*, *49*, e2022GL098242. https://doi.org/10.1029/2022GL098242

Received 25 FEB 2022
Accepted 27 MAY 2022

Abstract Approximately 1–3 violent tornadoes hit Europe each decade. We use the ERA5 reanalysis and WRF model to reconstruct environments for 12 cases between 1957 and 2021. Violent tornadoes in Europe occur in a variety of synoptic and mesoscale patterns, but they share environmental similarities with significant tornadoes from the United States. Downscaling simulations to 3 km grid-spacing showed the added value of improved resolution in representing local convective environments. In 8 out of 12 simulations, the model indicated updraft helicity (UH) tracks in a favorable convective environment in spatial (+/−50 km) and temporal (+/−3 hr) proximity to the tornado report. Tornadoes were accompanied by a mean 0–6 km wind shear of 24.3 m s^{-1} and mean convective available potential energy of 1678 J kg^{-1}. The combination of UH tracks with convective environments offers promising results for operational forecasting in Europe, and should be explored in future studies.

Plain Language Summary Violent tornadoes produce large societal impacts and considerable damage. Approximately 1–3 such events hit Europe each decade. In this study, we reconstruct the environmental conditions using the Weather Research and Forecasting model for 12 violent tornadoes in Europe from 1957 to 2021. We use metrics providing information about atmospheric instability and wind variability to analyze conditions under which these tornadoes formed. This helps to study events that occurred before the radar and satellite era when only limited information is available about them. In 8 out of 12 cases, the model successfully simulated storm tracks in a favorable tornado environment close to the location of the actual tornado report. Our results indicate the importance of performing high-resolution simulations in reconstructing tornado events, and they offer promising results in improving operational forecasting of tornadoes across Europe.

1. Introduction

Tornadoes in Europe have been evaluated in numerous case studies and regional climatologies. However, due to temporal and spatial inhomogeneities associated with their reporting, construction of reliable climatologies and risk estimation still poses a challenge (Antonescu et al., 2016; Chernokulsky, Kurgansky, et al., 2020; Grieser & Haines, 2020; Groenemeijer & Kühne, 2014). Interest in tornado research has significantly increased in the 21st century, but due to the lack of tornado reporting practices in many European countries, the tornado threat is still likely underestimated (Antonescu et al., 2017, 2018; Pîrloagă et al., 2021). Much higher efficiency in tornado reporting can be observed across highly populated Western and Central Europe (Groenemeijer et al., 2017; Taszarek, Allen, Groenemeijer, et al., 2020), where severe weather outbreaks often produce large societal impacts and considerable damage to infrastructure (Doswell, 2003; Grieser & Terenzi, 2016; Púčik et al., 2019).

Based on information available in the scientific literature and historical sources, it can be estimated that several violent tornadoes have occurred across Europe over the last 100 years (Antonescu et al., 2018; Holzer et al., 2018; Peterson, 1998; Taszarek & Gromadzki, 2017; Zanini et al., 2017). Analyzing historical tornadoes that occurred prior to radar or satellite measurements, and where limited information is available, is challenging. However, in such cases, it is possible to use numerical weather models to study atmospheric conditions in which tornadoes developed, and use those patterns to assess risks. For this purpose, reanalysis products have been widely used for the United States and Europe (Allen et al., 2018; Gensini & Brooks, 2018; Gensini & de Guenni, 2019; Taszarek, Allen, Púčik, et al., 2020, 2021). However, reanalyses feature limited grid spacing ranging typically from 2.5° to 0.25° and include convective parameterization. This resolution is sufficient to represent synoptic-scale

patterns, but cannot simulate mesoscale features well, especially over areas with complex orography (Rummukainen, 2015; Varga & Breuer, 2021). Reconstruction of storm tracks and mesoscale environments can be provided through dynamical downscaling with convective-allowing models, which has been commonly applied in the operational forecasting (Clark et al., 2012; Gallo et al., 2016, 2018) and climatological evaluations across the United States (Gensini & Mote, 2014; Hoogewind et al., 2017; Robinson et al., 2013; Trapp et al., 2011). In Europe, high-resolution simulations were performed for case studies of modern tornado events (Avolio & Miglietta, 2021; Chernokulsky, Shikhov, et al., 2020; Miglietta et al., 2017), but only Antonescu et al. (2020) focused on a simulation concerning a historical violent tornado outbreak.

As we believe that more attention should be devoted to reconstructing European violent tornado environments, we evaluate 12 such events between 1957 and 2021. For each case, we perform high-resolution simulations to compare simulated tracks of rotating updrafts with location and timing of tornado reports. In addition, we also analyze synoptic-scale patterns and proximity environments associated with violent tornadoes. While prior research evaluated European tornado events mainly with coarse-grid reanalyses (e.g., Coffer et al., 2020), here, we use high-resolution updraft helicity tracks (UH; Kain et al., 2010), which have been rarely applied in Europe. Despite rich literature from the United States on the utility of UH (Clark et al., 2013; Gallo et al., 2018, 2019; Sobash et al., 2011, 2019), only a very few European elaborations applied UH in case studies (e.g., Antonescu et al., 2020; Pilguj et al., 2019). In this context, we do believe that by testing UH for 12 violent tornado events, our work may have a positive impact on future studies covering similar topics in Europe, especially given that such extreme events were rarely studied outside the area of the United States.

2. Dataset and Methodology

2.1. Tornado Events

We used the European Severe Weather Database (ESWD; Dotzek et al., 2009) to choose 12 violent tornado events (F4 and F5 in Fujita scale; Fujita, 1971) between 1957 and 2021 and the area of 1°W–25°E and 40°N–55°N. This region will be the downscaling domain specified for this study (Figure 1). Due to domain limitations, the violent tornado from Ivanovo (Russia) on 9 June 1984 was not included (Chernokulsky & Shikhov, 2018). In addition to data provided in ESWD, we supplemented selected reports with additional information found in historical sources related to these events (Figure 1). Photographies showing violent tornado damage for selected cases are presented in Figure S1 of Supporting Information S1. We refer to each tornado by the year when it occurred. In 1967, two violent tornadoes were reported in France on the same day (Antonescu et al., 2018), and we consider them as one event.

2.2. WRF Simulations

Numerical simulations were performed with the Weather Research and Forecasting Model (WRF) version 4.2 (Skamarock et al., 2019), using pressure-level data from the ERA5 reanalysis (Hersbach et al., 2020) with 0.25° horizontal grid spacing as initial and lateral/boundary conditions. The model was configured with two one-way nested domains (Figure 1) with horizontal resolutions of 9 km (379 × 292 grid points) and 3 km (835 × 595 grid points). Vertically, both domains were configured for 45 levels up to 50 hPa. In model preprocessing, the domains were configured using a Lambert projection and Global Multi-resolution Terrain Elevation Data (Danielson & Gesch, 2011). The physics configuration includes the Thompson scheme (G. Thompson et al., 2008) for representation of microphysical processes, the Yonsei University Scheme (Hong et al., 2006) for planetary boundary layer, the Multi-scale Kain-Fritsch Scheme (Zheng et al., 2016) for cumulus physics in the outer domain, and Dudhia (1989) and RRTM (Mlawer et al., 1997) schemes for long- and shortwave radiation. In total, 12 simulations for each tornado event were performed for a period of 24 hr and an initialization time at 00 UTC.

2.3. Analyzed Parameters

To derive convective parameters from vertical profiles of pressure, altitude, temperature, humidity, U and V from ERA5 and WRF we used the *thundeR* R language package (Taszarek et al., 2021). We calculate parameters that are commonly used in the operational forecasting and climatological evaluations of significant tornadoes (Brooks

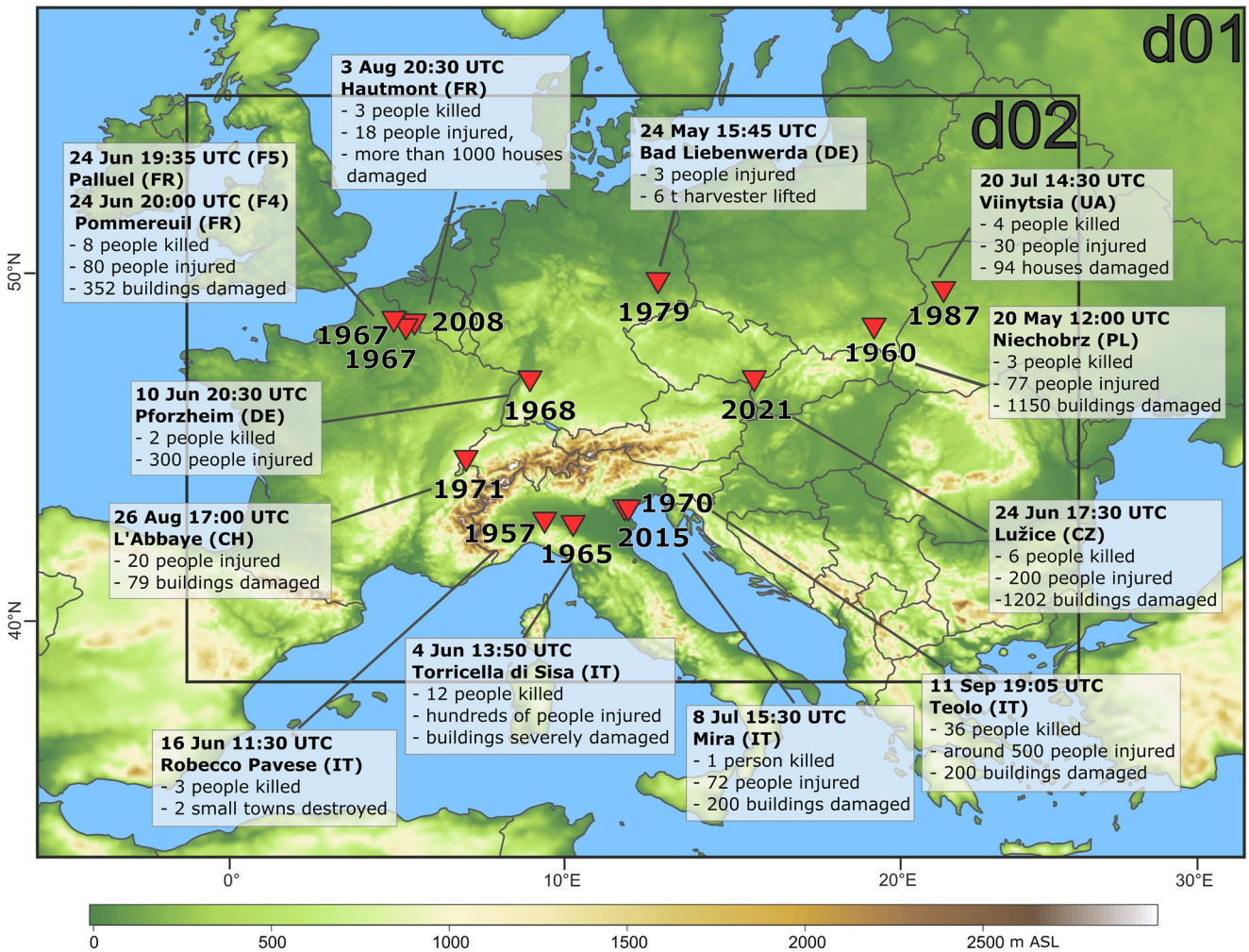

Figure 1. WRF model domains (d01, d02) and violent tornado events evaluated in this study. Photographies showing violent tornado damage for selected cases are presented in Figure S1 of Supporting Information S1.

et al., 2003; Grams et al., 2012; Gensini et al., 2021; Hua & Anderson-Frey, 2021; Ingrosso et al., 2020; R. L. Thompson et al., 2003, 2012, 2013; Taszarek, Allen, Púčik, et al., 2020). These include: convective available potential energy (CAPE), convective inhibition (CIN), 0–500 m mean mixing ratio (MIXR), lifted condensation level (LCL), 0–1 km vertical wind shear (S01), 0–6 km vertical wind shear (S06), 0–500 m storm-relative helicity (SRH), and the significant tornado parameter (STP; updated formula from Coffer et al. (2019) with effective SRH replaced by 0–500 m version). A mixed-layer (ML) of 0–500 m is used to calculate parcel thermodynamic parameters.

We use the 500 hPa geopotential height and wind from ERA5 to evaluate the synoptic setup at the time of the tornado event. Storm tracks from the WRF output are depicted using maximum hourly 2–5 km UH values. This parameter is the vertical integral of updraft's velocity and vorticity, and serves as a proxy for mid-level rotation in supercell thunderstorms (Kain et al., 2008, 2010). In the United States, it was noted that the best forecast performance was typically in situations when UH tracks were supported by favorable tornado background environments (Clark et al., 2012; Gallo et al., 2016, 2018; Sobash et al., 2016). For this reason, in this study we combine UH tracks with STP (maximum hourly values between 06 and 00 UTC) to evaluate their spatial agreement and compare with tornado reports. We also compare UH and convective precipitation over hourly steps within 50 km vicinity of the tornado report.

2.4. Pre-Convective Profiles

For each tornado event, we present Skew-T diagrams and hodographs from WRF and ERA5 composite mean profiles are available in Figures S2 and S3 of Supporting Information S1. To choose a representative WRF

profile and account for complex convective modes simulated in the model we perform a manual investigation of each case in the search of warm-sector inflow zones in the proximity of simulated convective cells or just before convective initiation (proximity of 100 km and 3 hr to tornado report). Only areas where composite reflectivity equaled 0 dBZ were considered. To account for a large spatial variability and possibility of single-grid profile contamination by nearby convective cells (Nowotarski & Markowski, 2016), we use all grids within a 15 km circle to calculate a mean profile (see Supporting Information S1 and Figure S4 in Supporting Information S1 for further details). Once a representative WRF profile is chosen, we match it with the equivalent ERA5 profile. For both WRF and ERA5 we use model levels (instead of fewer pressure levels) to ensure the highest available vertical resolution is used to calculate convective parameters.

3. Results and Discussion

3.1. Synoptic and Mesoscale Environment

Violent tornadoes in Europe occurred in a variety of synoptic patterns (Figure 2). However, they typically shared a common feature of a high horizontal geopotential gradient under an area of enhanced instability (except low-CAPE cases in 1960 and 2008). The majority of events were accompanied by mid-tropospheric southwesterly flow, while two had southern (1957, 1979) and another two western (2008, 2015) advection components. Tornado reports were typically located in the warm sector on the eastern flank of the approaching trough, often in the area of upper level divergence. Such patterns are in agreement with the conceptual models of the synoptic setting for severe storms, and similar to those associated with tornado outbreaks across the United States (Knupp et al., 2014; Mercer et al., 2012; Tochimoto & Niino, 2016, 2017). However, as shown in Taszarek, Allen, Púčik, et al. (2020) tornadoes in Europe typically feature lower mid-tropospheric temperature lapse rates, moisture content, instability and vertical wind shear and thus, are less common compared to the United States where high-CAPE and high-shear situations are more frequent. Such scenarios are rare in Europe and typically associated with the 'Spanish Plume' setup displacing elevated mixed-layer from the Iberian Peninsula into Western and Central Europe (Hamid, 2012; Mathias et al., 2017; van Delden, 2001) or situations when moisture is locked by the Alps in northern Italy (Bagaglini et al., 2021).

We also note that two violent tornadoes in Europe occurred in a high-shear and low-CAPE (HSLC) environment as was the case for 1960 and 2008 (Wesolek & Mahieu, 2011). Such environments are typically responsible for severe weather outbreaks during the cold season (Mathias et al., 2019; Sherburn & Parker, 2014; Sherburn et al., 2016; van den Broeke et al., 2005) and are often accompanied by a strong synoptic-scale lift (as was the case in 2008). HSLC tornadoes can occur both within supercell and non-supercell small scale mesovortices and their operational forecasting is very challenging (Anderson-Frey et al., 2016, 2017; Davis & Parker, 2014; Šinger & Púčik, 2020).

Proximal vertical wind profiles derived from WRF and ERA5 indicate that in nearly every case, tornadoes were associated with clockwise curved hodographs and high near-ground helicity with SRH values of more than 70 $m^2\ s^{-2}$ in 8 out of 12 simulations (Figure 3). The right-moving supercell storm motion vector (Bunkers et al., 2000) indicated thunderstorm movement direction ranging from northeast to east. Hodograph curvature was enhanced in WRF compared to equivalent ERA5 profiles with a mean SRH of 92 and 62 $m^2\ s^{-2}$ respectively (Figure 3b). However, for both databases, we found a mean value of around 24 m s^{-1} for S06 and around 9 m s^{-1} for S01. No large differences were found for LCL, which for both WRF and ERA5 was approximately 1,000 m AGL, consistent with the significant tornado environments in Europe evaluated by Coffer et al. (2020). WRF and ERA5 were similar for the mean vertical profiles of air temperature, with both datasets indicating steep lapse rates (Figure 3a). Larger variability was observed for dew point, but with a general agreement between ERA5 and WRF for the mean profiles (Figure 3b). Tornadoes were typically accompanied by rich boundary layer's moisture (mean MIXR for both ERA5 and WRF of 12.6 g kg^{-1}) and moderate instability (mean CAPE around 1650 J kg^{-1}). However, variability in CAPE was large as it ranged from 100–300 J kg^{-1} in 2008 up to 2500–3500 J kg^{-1} in 2021, indicating that violent tornadoes can form in a variety of thermodynamic environments. Contrary, S06 was generally enhanced in every case. A weaker resistance to convective initiation with a mean CIN of around −30 J kg^{-1} was also observed.

Overall, mean values of convective parameters for European violent tornadoes presented in Figure 3b are similar to medians obtained for significant tornadoes across the United States by R. L. Thompson et al. (2003). For this

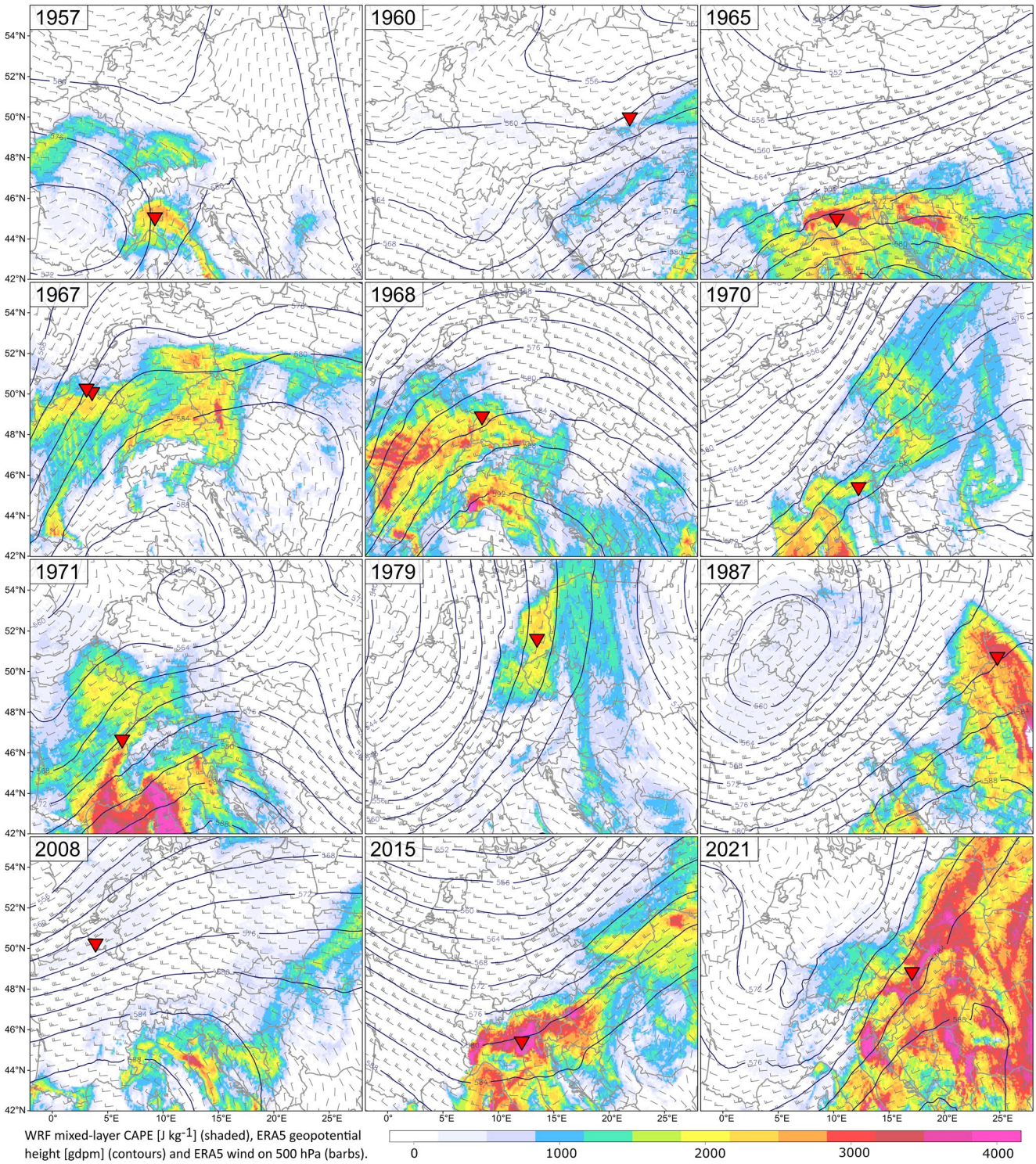

Figure 2. Maximum 06–00 UTC ML CAPE (shaded), 500 hPa geopotential height (contour lines) and 500 hPa wind (barbs). Red triangles denote location of violent tornado events.

reason, the STP (originally designed to forecast significant tornadoes in the United States) seems to work for violent tornado events in Europe as well. Mean STP for all violent tornado cases evaluated was 0.9 for WRF and 0.7 for ERA5, which exceeded the mean value of 0.15 for significant tornado events in Europe found with ERA5 in Coffer et al. (2020) and Taszarek, Allen, Púčik, et al. (2020).

a

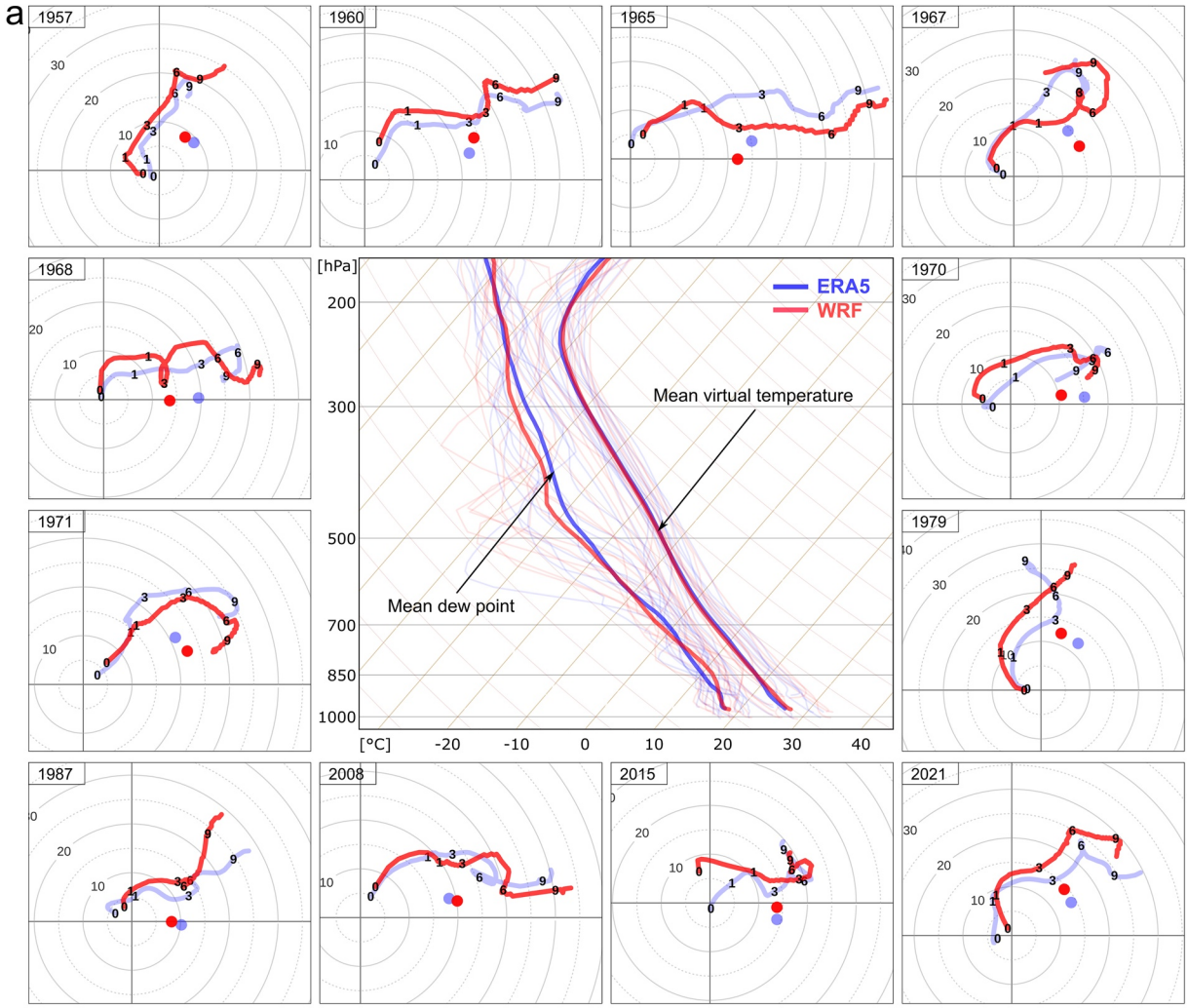

b

Year	S01 [m s^{-1}]		S06 [m s^{-1}]		SRH [m^{2}s^{-2}]		LCL [m AGL]		MIXR [g kg^{-1}]		CAPE [J kg^{-1}]		CIN [J kg^{-1}]		STP	
	ERA5	WRF	ERA5	WRF	ERA5	WRF	ERA5	WRF	ERA5	WRF	ERA5	WRF	ERA5	WRF	ERA5	WRF
1957	3.8	5.0	17.6	21.9	8	17	690	580	12.5	13.9	1125	2276	-2	0	0.1	0.3
1960	11.9	8.6	29.1	26.6	119	121	520	975	10.6	10.2	508	896	0	0	0.6	1.2
1965	16.6	10.4	39.4	38.6	122	78	600	620	13.2	12.8	2027	1615	-56	-23	3.2	1.7
1967	10.2	12.6	23.0	22.7	118	172	1225	1300	12.5	11.2	1968	701	-25	-88	1.8	0.6
1968	8.2	12.1	29.4	25.0	97	134	1645	1320	12.4	12.9	1629	2042	-45	-41	0.7	1.8
1970	7.7	8.4	26.1	24.1	22	90	1200	1135	12.3	13.0	654	1069	-172	-131	0.0	0.4
1971	11.1	9.8	25.3	26.0	27	75	1025	655	10.3	11.8	1078	1805	-22	0	0.3	1.5
1979	7.1	9.1	19.9	22.0	42	65	1165	1045	9.9	10.8	1448	1720	-14	-4	0.4	1.0
1987	5.5	3.4	16.8	12.9	21	26	1100	1425	14.5	14.3	2257	2603	-35	-7	0.3	0.2
2008	14.2	14.1	22.6	26.2	137	185	490	530	11.8	11.8	136	299	-22	-9	0.0	0.5
2015	6.8	11.1	20.0	19.0	28	73	1010	1405	16.6	15.1	3009	2439	-27	-47	0.8	0.9
2021	7.7	7.3	25.6	26.8	4	68	1200	1740	15.2	12.8	3544	2672	-5	-5	0.1	0.5
Mean	**9.2**	**9.3**	**24.6**	**24.3**	**62**	**92**	**989**	**1061**	**12.7**	**12.6**	**1615**	**1678**	**-35**	**-29**	**0.7**	**0.9**

Figure 3. Pre-convective profiles with hodographs (a) and equivalent convective parameters (b) for tornado events derived from WRF (red) and ERA5 (blue). The right-moving supercell storm motion is represented with a point.

Tornadoes in 1957, 1965, 1968, 2015 and 2021 developed in rare (for Europe) high-shear (>20 m s^{-1}) and high-CAPE (>2,000 J kg^{-1}) situations, comparable to conditions for significant tornadic supercells across the Great Plains of the United States (Anderson-Frey & Brooks, 2021; Coffer et al., 2017, 2019; Coniglio & Parker, 2020; Nixon & Allen, 2021). Mean hodographs presented by Coffer et al. (2020) indicated that European significant tornadoes had a much weaker southerly wind component and less curvature in the lowest 3 km compared to the United States. However, violent tornado hodographs presented in this study (especially for WRF; Figure 3a) seem to be more comparable to those presented in Coffer et al. (2020) and Nixon and Allen (2021).

3.2. Simulated Storm Tracks

In all situations, WRF simulated convective initiation in both spatial (+/−50 km) and temporal (+/−3h) proximity to the tornado reports (Figures 4 and 5). However, convection was not associated with rotating updrafts in every case. Long and isolated UH tracks were in good agreement with the tornado events of 1960, 1979, 2021. These cases were supported by no less than 22 m s^{-1} of S06 and 65 m^2 s^{-2} of SRH in WRF (Figure 3b). Long and strong UH tracks with good temporal timing, but slight spatial displacement were simulated by WRF for the cases of 1965, 1967, and 1971, all of them with S06 no lower than 22 m s^{-1}. Similar UH signals for the tornadoes of 1967 were obtained by Antonescu et al. (2018), but with ERA-40 initial conditions and 800 m grid spacing. A strong signal of UH exceeding 100 m^2 s^{-2} in the vicinity of the tornado report but with a less organized convective mode and smaller coverage of storms was observed for the tornado cases of 1957 and 1987. Both of these events were accompanied by smaller S06 of around 17 m s^{-1} based on ERA5. In 1968, a strong signal from UH was shifted by more than 6 hr backward. The tornado cases of 1970 and 2015 were poorly captured by UH in terms of both temporal and spatial patterns (Figures 4 and 5). Interestingly, both of these events occurred in a similar location close to the shoreline of the Adriatic Sea. We hypothesize that these events may be related to storms interacting with sea breeze boundaries, which is a more localized phenomena and thus less predictable than the events driven by favorable larger scale environmental conditions. The area of northern Italy features very complex orography that could also be a contributing factor.

A HSLC violent tornado event of 2008 featuring only 100–300 J kg^{-1} of CAPE but large S01 of 14 m s^{-1} (Figure 3b) was the only case where no tracks of UH exceeding 40 m^2 s^{-2} were produced in the simulation. WRF indicated multiple shallow convective cells in the temporal and spatial vicinity of the tornado report, but with insignificant rotation in the UH layer of 2–5 km. This result is unsurprising as high-resolution simulations in the HSLC environments have been shown to demonstrate large uncertainty in predicting storm intensity (Lawson, 2019). Sobash et al. (2016) also noted that shallower layers of UH such as 0–3 km AGL should be used in forecasting HSLC tornadoes compared to the 2–5 km version used in our study that works well for warm season events. Wade and Parker (2021) explained that supercells in HSLC environments reach their largest vertical velocities from dynamic perturbation pressure gradient accelerations that are maximized at low-levels, instead of accelerations resulting from buoyancy that are dominant in high-CAPE environments. Such events pose a big challenge in their forecasting, as metrics that work well in high-CAPE situations are less skillful in HSLC (Anderson-Frey et al., 2016). This was also noted by Sherburn and Parker (2014), who suggested that composite parameters such as STP should be used with lower operational thresholds in HSLC environments. Warm season events in our study were typically accompanied by enhanced STP values, which in combination with simulated UH tracks allowed to indicate areas with a tornado threat (Figure 4).

4. Conclusions

In this work, we showed that violent tornadoes in Europe can occur in a variety of synoptic and mesoscale patterns, which makes their forecasting challenging, especially given the unique mesoscale interactions with complex European orography. In the environmental context, we found that violent tornadoes in Europe share similarities with significant tornadoes in the United States. Downscaling simulations showed the added value of improved resolution in representing local convective environments, a result consistent with Varga and Breuer (2021). We also observed that the downscaling effect led to more favorable tornado environments with enhancements in SRH and STP compared to initial ERA5 conditions. In 8 out of 12 simulations, WRF indicated UH tracks within a favorable convective environment in both spatial and temporal proximity to the violent tornado report. In one case a large temporal shift occurred while in three others the UH signal was too weak. We noticed that long UH tracks were

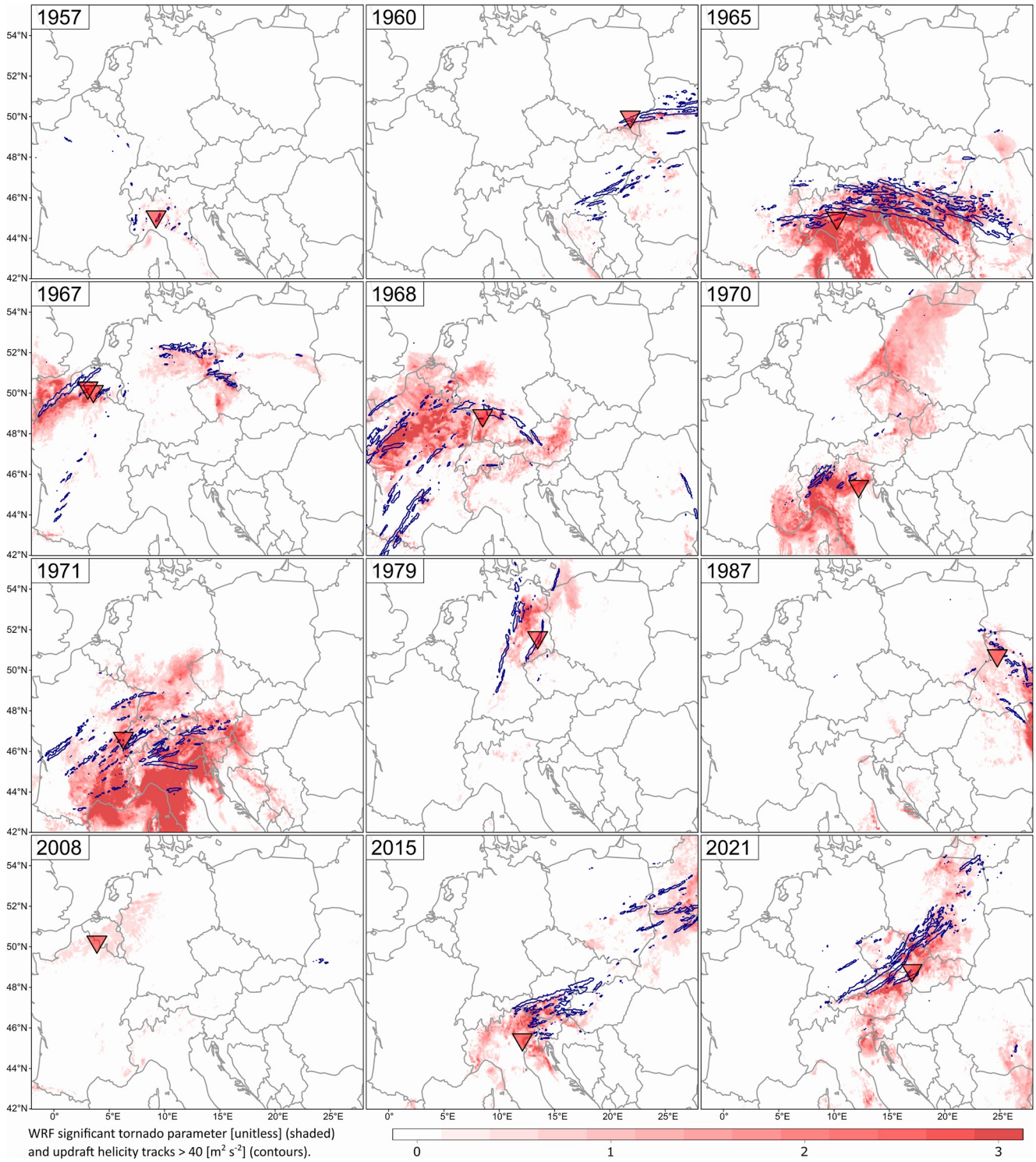

Figure 4. Maximum 06–00 UTC STP (shaded) and UH > 40 $m^2 s^{-2}$ tracks (contour lines). Red triangles denote location of violent tornado events.

typically associated with S06 of at least 22 m s^{-1} while lower shear environments resulted in weaker UH signals. However, due to the limited sample size evaluated in this study, these results should be interpreted with caution.

A technique combining UH tracks from high-resolution simulations with environmental values of STP (or other convective parameters) should be further explored. While in the United States, similar techniques have

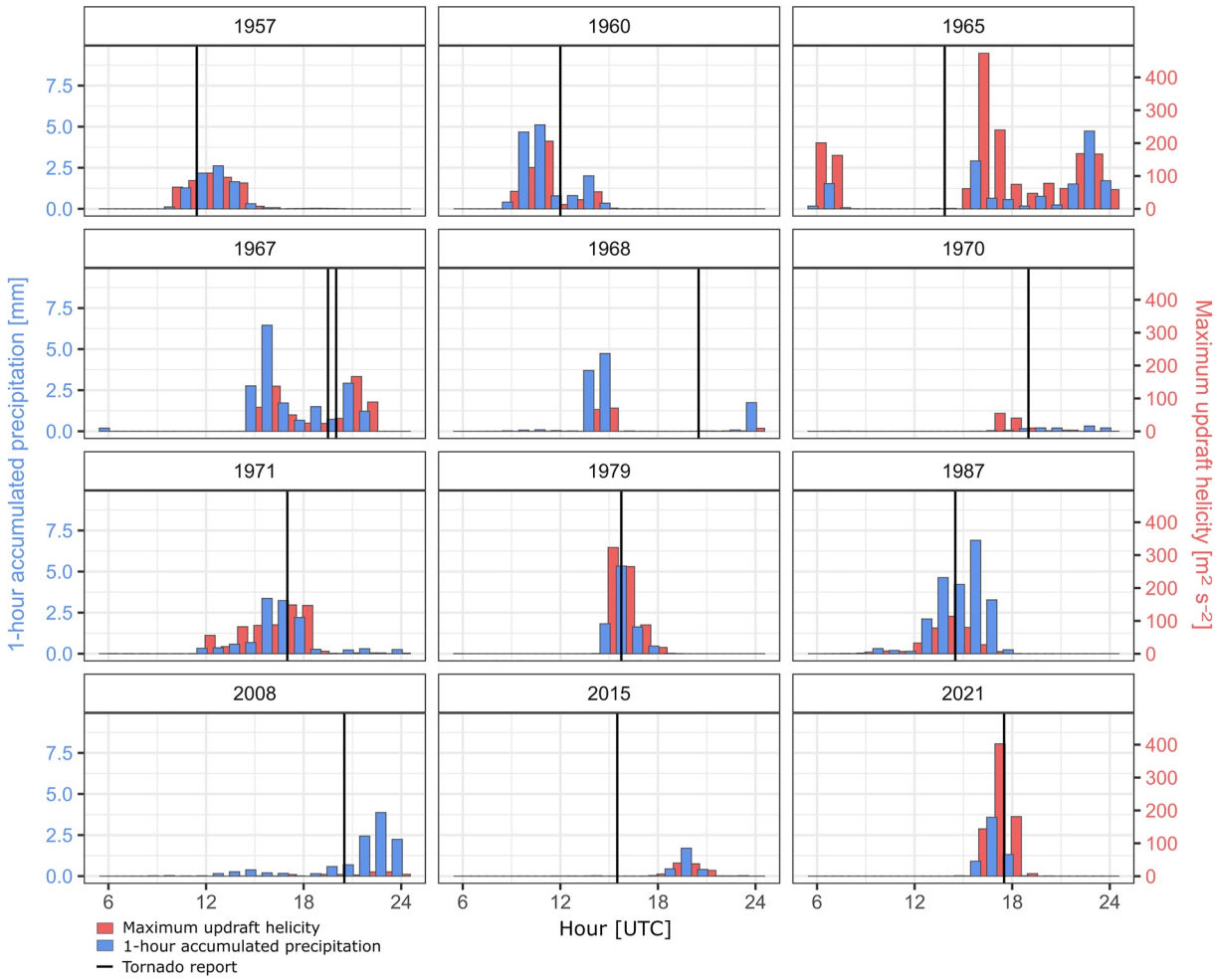

Figure 5. Mean 1-hr accumulated precipitation (blue) and maximum 1-hr updraft helicity (red) within 50 km proximity of the tornado report. A vertical black line denotes the time of the tornado.

been applied operationally with ensemble-based approaches (Clark et al., 2012; Gallo et al., 2016, 2018, 2019; Loken et al., 2017; Trier et al., 2021), very little is known about tornado forecasting performance in Europe. As evidenced in our study, despite a variety of synoptic patterns and types of convective environments, in the majority of cases, UH track near the location of the tornado report was associated with climatologically enhanced values of STP. While this does not necessarily translate into a skillful prediction technique of violent tornado events in Europe, it offers promising results that should be further explored in future research, especially involving ensemble-based approach and background climatology covering a period of a few decades. Increasing resolution from 3 to 1 km and focusing on low-level UH is another opportunity in which tornado forecasts could be improved (Sobash et al., 2019). As severe storms with significant tornadoes happen regularly in Europe and their threat is likely underestimated (Antonescu et al., 2017, 2020), this topic requires more attention from researchers and decision makers.

Data Availability Statement

Numerical simulations were performed using WRF4.2.1, which can be downloaded from the UCAR website (https://www2.mmm.ucar.edu/wrf/users/download/get_source.html). European tornado reports are available at European Severe Weather Database (https://eswd.eu/). ERA5 data were downloaded from the European Centre for Medium-Range Weather Forecasts (ECMWF), Copernicus Climate Change Service (C3S) at Climate Data Store (CDS). ERA5 is available at https://cds.climate.copernicus.eu/cdsapp#!/dataset/reanalysis-era5-pres-

sure-levels-preliminary-back-extension, https://cds.climate.copernicus.eu/cdsapp#!/dataset/reanalysis-era5-pressure-levels (pressure levels) and https://cds.climate.copernicus.eu/cdsapp#!/dataset/reanalysis-era5-single-levels-preliminary-back-extension, https://cds.climate.copernicus.eu/cdsapp#!/dataset/reanalysis-era5-single-levels (single levels).

Acknowledgments
Funding was provided by the Polish National Science Centre (2019/33/N/ST10/00403 and 2020/39/D/ST10/00768), and the Polish National Agency for Academic Exchange—the Iwanowska Programme (PPN/IWA/2019/1/00148). The WRF simulations were carried out using resources provided by the Wroclaw Centre for Networking and Supercomputing (http://wcss.pl), Grant No. 170.

References

Allen, J. T., Molina, M. J., & Gensini, V. A. (2018). Modulation of annual cycle of tornadoes by El Niño–southern Oscillation. *Geophysical Research Letters*, *45*(11), 5708–5717. https://doi.org/10.1029/2018GL077482

Anderson-Frey, A. K., & Brooks, H. (2021). Compared to what? Establishing environmental baselines for tornado warning skill. *Bulletin of the American Meteorological Society*, *102*(4), E738–E747. https://doi.org/10.1175/BAMS-D-19-0310.1

Anderson-Frey, A. K., Richardson, Y. P., Dean, A. R., Thompson, R. L., & Smith, B. T. (2016). Investigation of near-storm environments for tornado events and warnings. *Weather and Forecasting*, *31*(6), 1771–1790. https://doi.org/10.1175/WAF-D-16-0046.1

Anderson-Frey, A. K., Richardson, Y. P., Dean, A. R., Thompson, R. L., & Smith, B. T. (2017). Self-organizing maps for the investigation of tornadic near-storm environments. *Weather and Forecasting*, *32*(4), 1467–1475. https://doi.org/10.1175/WAF-D-17-0034.1

Antonescu, B., Fairman, J. G., Jr., & Schultz, D. M. (2018). What is the worst that could happen? Reexamining the 24–25 June 1967 tornado outbreak over Western Europe. *Weather, Climate, and Society*, *10*(2), 323–340. https://doi.org/10.1175/WCAS-D-17-0076.1

Antonescu, B., Púčik, T., & Schultz, D. M. (2020). Hindcasting the first tornado forecast in Europe: 25 June 1967. *Weather and Forecasting*, *35*(2), 417–436. https://doi.org/10.1175/WAF-D-19-0173.1

Antonescu, B., Schultz, D. M., Holzer, A., & Groenemeijer, P. (2017). Tornadoes in Europe: An underestimated threat. *Bulletin of the American Meteorological Society*, *98*(4), 713–728. https://doi.org/10.1175/BAMS-D-16-0171.1

Antonescu, B., Schultz, D. M., Lomas, F., & Kühne, T. (2016). Tornadoes in Europe: Synthesis of observational datasets. *Monthly Weather Review*, *144*(7), 2445–2480. https://doi.org/10.1175/MWR-D-15-0298.1

Avolio, E., & Miglietta, M. M. (2021). Multiple tornadoes in the Italian Ionian regions: Observations, sensitivity tests and mesoscale analysis of convective storm environmental parameters. *Atmospheric Research*, *263*, 105800. https://doi.org/10.1016/j.atmosres.2021.105800

Bagaglini, L., Ingrosso, R., & Miglietta, M. M. (2021). Synoptic patterns and mesoscale precursors of Italian tornadoes. *Atmospheric Research*, *253*, 105503. https://doi.org/10.1016/j.atmosres.2021.105503

Brooks, H. E., Lee, J. W., & Craven, J. P. (2003). The spatial distribution of severe thunderstorm and tornado environments from global reanalysis data. *Atmospheric Research*, *67*(68), 73–94. https://doi.org/10.1016/S0169-8095(03)00045-0

Bunkers, M. J., Klimowski, B. A., Zeitler, J. W., Thompson, R. L., & Weisman, M. L. (2000). Predicting supercell motion using a new hodograph technique. *Weather and Forecasting*, *15*(1), 61–79. https://doi.org/10.1175/1520-0434(2000)015<0061:psmuan>2.0.co;2

Chernokulsky, A., Kurgansky, M., Mokhov, I., Shikhov, A., Azhigov, I., Selezneva, E., et al. (2020). Tornadoes in Northern Eurasia: From the middle age to the information era. *Monthly Weather Review*, *148*(8), 3081–3110. https://doi.org/10.1175/MWR-D-19-0251.1

Chernokulsky, A., & Shikhov, A. (2018). 1984 Ivanovo tornado outbreak: Determination of actual tornado tracks with satellite data. *Atmospheric Research*, *207*, 111–121. https://doi.org/10.1016/j.atmosres.2018.02.011

Chernokulsky, A., Shikhov, A., Bykov, A., & Azhigov, I. (2020). Satellite-based study and numerical forecasting of two tornado outbreaks in the Ural Region in June 2017. *Atmosphere*, *11*(11), 1146. https://doi.org/10.3390/atmos11111146

Clark, A. J., Gao, J., Marsh, P. T., Smith, T., Kain, J. S., Correia, J., Jr., et al. (2013). Tornado pathlength forecasts from 2010 to 2011 using ensemble updraft helicity. *Weather and Forecasting*, *28*(7), 387–407. https://doi.org/10.1175/WAF-D-12-00038.1

Clark, A. J., Kain, J. S., Marsh, P. T., Correia, J., Jr., Xue, M., & Kong, F. (2012). Forecasting tornado path lengths using a three-dimensional object identification algorithm applied to convection-allowing forecasts. *Weather and Forecasting*, *27*(5), 1090–1113. https://doi.org/10.1175/WAF-D-11-00147.1

Coffer, B. E., Parker, M. D., Dahl, J. M. L., Wicker, L. J., & Clark, A. J. (2017). Volatility of tornadogenesis: An ensemble of simulated nontornadic and tornadic supercells in VORTEX2 environments. *Monthly Weather Review*, *145*(11), 4605–4625. https://doi.org/10.1175/MWR-D-17-0152.1

Coffer, B. E., Parker, M. D., Thompson, R. L., Smith, B. T., & Jewell, R. E. (2019). Using near-ground storm relative helicity in supercell tornado forecasting. *Weather and Forecasting*, *34*(5), 1417–1435. https://doi.org/10.1175/WAF-D-19-0115.1

Coffer, B. E., Taszarek, M., & Parker, M. D. (2020). Near-ground wind profiles of tornadic and nontornadic environments in the United States and Europe from ERA5 reanalyses. *Weather and Forecasting*, *35*(6), 2621–2638. https://doi.org/10.1175/WAF-D-20-0153.1

Coniglio, M. C., & Parker, M. D. (2020). Insights into supercells and their environments from three decades of targeted radiosonde observations. *Monthly Weather Review*, *148*(12), 4893–4915. https://doi.org/10.1175/mwr-d-20-0105.1

Danielson, J. J., & Gesch, D. B. (2011). Global multi-resolution terrain elevation data 2010 (GMTED2010). Report No. *OFR 2011–1073* 26. https://doi.org/10.3133/ofr20111073

Davis, J. M., & Parker, M. D. (2014). Radar climatology of tornadic and nontornadic vortices in high-shear, low-CAPE environments in the mid-Atlantic and southeastern United States. *Weather and Forecasting*, *29*(4), 828–853. https://doi.org/10.1175/WAF-D-13-00127.1

Doswell, C. A., III. (2003). Societal impacts of severe thunderstorms and tornadoes: Lessons learned and implications for Europe. *Atmospheric Research*, *67*(68), 135–152. https://doi.org/10.1016/S0169-8095(03)00048-6

Dotzek, N., Groenemeijer, P., Feuerstein, B., & Holzer, A. M. (2009). Overview of ESSL's severe convective storms research using the European Severe Weather Database ESWD. *Atmospheric Research*, *93*(1–3), 575–586. https://doi.org/10.1016/j.atmosres.2008.10.020

Dudhia, J. (1989). Numerical study of convection observed during the Winter Monsoon Experiment using a mesoscale two–dimensional model. *Journal of the Atmospheric Sciences*, *46*(20), 3077–3107. https://doi.org/10.1175/1520-0469(1989)046<3077:nsocod>2.0.co;2

Fujita, T. T. (1971). Proposed characterization of tornadoes and hurricanes by area and intensity. *SMRP Research Paper No. 91*, (p.42). University of Chicago.

Gallo, B. T., Clark, A. J., & Dembek, S. R. (2016). Forecasting tornadoes using convection-permitting ensembles. *Weather and Forecasting*, *31*(1), 273–295. https://doi.org/10.1175/WAF-D-15-0134.1

Gallo, B. T., Clark, A. J., Smith, B. T., Thompson, R. L., Jirak, I., & Dembek, S. R. (2018). Blended probabilistic tornado forecasts: Combining climatological frequencies with NSSL–WRF ensemble forecasts. *Weather and Forecasting*, *33*(2), 443–460. https://doi.org/10.1175/WAF-D-17-0132.1

Gallo, B. T., Clark, A. J., Smith, B. T., Thompson, R. L., Jirak, I., & Dembek, S. R. (2019). Incorporating UH occurrence time to ensemble-derived tornado probabilities. *Weather and Forecasting*, *34*(1), 151–164. https://doi.org/10.1175/WAF-D-18-0108.1

Gensini, V. A., & Brooks, H. E. (2018). Spatial trends in United States tornado frequency. *NPJ Climate and Atmospheric Science*, *1*, 38. https://doi.org/10.1038/s41612-018-0048-2

Gensini, V. A., Converse, C., Ashley, W. S., & Taszarek, M. (2021). Machine learning classification of significant tornadoes and hail in the U.S. using ERA5 proximity soundings. *Weather and Forecasting*, *36*(6), 2143–2160. https://doi.org/10.1175/WAF-D-21-0056.1

Gensini, V. A., & de Bravo Guenni, L. (2019). Environmental covariate representation of seasonal US tornado frequency. *Journal of Applied Meteorology and Climatology*, *58*(6), 1353–1367. https://doi.org/10.1175/JAMC-D-18-0305.1

Gensini, V. A., & Mote, T. L. (2014). Estimations of hazardous convective weather in the United States using dynamical downscaling. *Journal of Climate*, *27*(17), 6581–6589. https://doi.org/10.1175/JCLI-D-13-00777.1

Grams, J. S., Thompson, R. L., Snively, D. V., Prentice, J. A., Hodges, G. M., & Reames, L. J. (2012). A climatology and comparison of parameters for significant tornado events in the United States. *Weather and Forecasting*, *27*(1), 106–123. https://doi.org/10.1175/WAF-D-11-00008.1

Grieser, J., & Haines, P. (2020). Tornado risk climatology in Europe. *Atmosphere*, *11*(7), 768. https://doi.org/10.3390/atmos11070768

Grieser, J., & Terenzi, F. (2016). Modeling financial losses resulting from tornadoes in European countries. *Weather, Climate, and Society*, *8*(4), 313–326. https://doi.org/10.1175/WCAS-D-15-0036.1

Groenemeijer, P., & Kühne, T. (2014). A climatology of tornadoes in Europe: Results from the European severe weather database. *Monthly Weather Review*, *142*(12), 4775–4790. https://doi.org/10.1175/MWR-D-14-00107.1

Groenemeijer, P., Púčik, T., Holzer, A. M., Antonescu, B., Riemann-Campe, K., Schultz, D. M., et al. (2017). Severe convective storms in Europe: Ten years of research and education at the European Severe Storms Laboratory. *Bulletin of the American Meteorological Society*, *98*(12), 2641–2651. https://doi.org/10.1175/BAMS-D-16-0067.1

Hamid, K. (2012). Investigation of the passage of a derecho in Belgium. *Atmospheric Research*, *107*, 86–105. https://doi.org/10.1016/j.atmosres.2011.12.013

Hersbach, H., Bell, B., Berrisford, P., Hirahara, S., Horányi, A., Muñoz-Sabater, J., et al. (2020). The ERA5 global reanalysis. *Quarterly Journal of Royal Meteorological Society*, *146*(730), 1999–2049. https://doi.org/10.1002/qj.3803

Holzer, A., Schreiner, T. M. E., & Púčik, T. (2018). A forensic re-analysis of one of the deadliest European tornadoes. *Natural Hazards and Earth System Sciences*, *18*, 1555–1565. https://doi.org/10.5194/nhess-18-1555-2018

Hong, S.-Y., Noh, Y., & Dudhia, J. (2006). A new vertical diffusion package with an explicit treatment of entrainment processes. *Monthly Weather Review*, *134*(9), 2318–2341. https://doi.org/10.1175/MWR3199.1

Hoogewind, K. A., Baldwin, M. E., & Trapp, R. J. (2017). The impact of climate change on hazardous convective weather in the United States: Insight from high-resolution dynamical downscaling. *Journal of Climate*, *30*(24), 10081–10100. https://doi.org/10.1175/JCLI-D-16-0885.1

Hua, Z., & Anderson-Frey, A. K. (2021). Self-organizing maps for the classification of spatial and temporal variability of tornado-favorable parameters. *Monthly Weather Review*, *150*(2), 393–407. https://doi.org/10.1175/MWR-D-21-0168.1

Ingrosso, R., Lionello, P., Miglietta, M. M., & Salvadori, G. (2020). A statistical investigation of mesoscale precursors of significant tornadoes: The Italian case study. *Atmosphere*, *11*(3), 301. https://doi.org/10.3390/atmos11030301

Kain, J. S., Dembek, S. R., Weiss, S. J., Case, J. L., Levit, J. J., & Sobash, R. A. (2010). Extracting unique information from high resolution forecast models: Monitoring selected fields and phenomena every time step. *Weather and Forecasting*, *25*(5), 1536–1542. https://doi.org/10.1175/2010WAF2222430.1

Kain, J. S., Weiss, S. J., Bright, D. R., Baldwin, M. E., Levit, J. J., Carbin, G. W., et al. (2008). Some practical considerations regarding horizontal resolution in the first generation of operational convection-allowing NWP. *Weather and Forecasting*, *23*(5), 931–952. https://doi.org/10.1175/WAF2007106.1

Knupp, K. R., Murphy, T. A., Coleman, T. A., Wade, R. A., Mullins, S. A., Schultz, C. J., et al. (2014). Meteorological overview of the devastating 27 April 2011 tornado outbreak. *Bulletin of the American Meteorological Society*, *95*(7), 1041–1062. https://doi.org/10.1175/BAMS-D-11-00229.1

Lawson, J. R. (2019). Predictability of idealized thunderstorms in buoyancy-shear space. *Journal of the Atmospheric Sciences*, *76*(9), 2653–2672. https://doi.org/10.1175/JAS-D-18-0218.1

Loken, E. D., Clark, A. J., Xue, M., & Kong, F. (2017). Comparison of next-day probabilistic severe weather forecasts from coarse-and fine-resolution CAMs and a convection-allowing ensemble. *Weather and Forecasting*, *32*(4), 1403–1421. https://doi.org/10.1175/WAF-D-16-0200.1

Mathias, L., Ermert, V., Kelemen, F. D., Ludwig, P., & Pinto, J. G. (2017). Synoptic analysis and hindcast of an intense bow echo in Western Europe: The 9 June 2014 storm. *Weather and Forecasting*, *32*(3), 1121–1141. https://doi.org/10.1175/WAF-D-16-0192.1

Mathias, L., Ludwig, P., & Pinto, J. G. (2019). Synoptic-scale conditions and convection-resolving hindcast experiments of a cold-season derecho on 3 January 2014 in Western Europe. *Natural Hazards and Earth System Sciences*, *19*(5), 1023–1040. https://doi.org/10.5194/nhess-19-1023-2019

Mercer, A. E., Shafer, C. M., Doswell, C. A., Leslie, L. M., & Richman, M. B. (2012). Synoptic composites of tornadic and nontornadic outbreaks. *Monthly Weather Review*, *140*(8), 2590–2608. https://doi.org/10.1175/MWR-D-12-00029.1

Miglietta, M. M., Mazon, J., & Rotunno, R. (2017). Numerical simulations of a tornadic supercell over the Mediterranean. *Weather and Forecasting*, *32*(3), 1209–1226. https://doi.org/10.1175/WAF-D-16-0223.1

Mlawer, E. J., Taubman, S. J., Brown, P. D., Iacono, M. J., & Clough, S. A. (1997). Radiative transfer for inhomogeneous atmospheres: RRTM, a validated correlated–k model for the longwave. *Journal of Geophysical Research*, *102*(D14), 16663–16682. https://doi.org/10.1029/97JD00237

Nixon, C. J., & Allen, J. T. (2021). Anticipating deviant tornado motion using a simple hodograph technique. *Weather and Forecasting*, *36*(1), 219–235. https://doi.org/10.1175/WAF-D-20-0056.1

Nowotarski, C. J., & Markowski, P. M. (2016). Modifications to the near-storm environment induced by simulated supercell thunderstorms. *Monthly Weather Review*, *144*(1), 273–293. https://doi.org/10.1175/MWR-D-15-0247.1

Peterson, R. E. (1998). A historical review of tornadoes in Italy. *Journal of Wind Engineering and Industrial Aerodynamics*, *74–76*, 123–130. https://doi.org/10.1016/S0167-6105(98)00010-5

Pilguj, N., Taszarek, M., Pajurek, Ł., & Kryza, M. (2019). High-resolution simulation of an isolated tornadic supercell in Poland on 20 June 2016. *Atmospheric Research*, *218*, 145–159. https://doi.org/10.1016/j.atmosres.2018.11.017

Pîrloagă, R., Ene, D., & Antonescu, B. (2021). Population bias on tornado reports in Europe. *Applied Sciences*, *11*(23), 11485. https://doi.org/10.3390/app112311485

Púčik, T., Castellano, C., Groenemeijer, P., Kühne, T., Rädler, A. T., Antonescu, B., & Faust, E. (2019). Large hail incidence and its economic and societal impacts across Europe. *Monthly Weather Review*, *147*(11), 3901–3916. https://doi.org/10.1175/MWR-D-19-0204.1

Robinson, E. D., Trapp, R. J., & Baldwin, M. E. (2013). The geospatial and temporal distributions of severe thunderstorms from high-resolution dynamical downscaling. *Journal of Applied Meteorology and Climatology*, *52*(9), 2147–2161. https://doi.org/10.1175/JAMC-D-12-0131.1

Rummukainen, M. (2015). Added value in regional climate modeling. *Wiley Interdisciplinary Reviews: Climate Change*, *7*(1), 145–159. https://doi.org/10.1002/wcc.378

Sherburn, K. D., & Parker, M. D. (2014). Climatology and ingredients of significant severe convection in high-shear, low-CAPE environments. *Weather and Forecasting*, *29*(4), 854–877. https://doi.org/10.1175/WAF-D-13-00041.1

Sherburn, K. D., Parker, M. D., King, J. R., & Lackmann, G. M. (2016). Composite environments of severe and nonsevere high-shear, low-CAPE convective events. *Weather and Forecasting*, *31*(6), 1899–1927. https://doi.org/10.1175/WAF-D-16-0086.1

Šinger, M., & Púčik, T. (2020). A challenging tornado forecast in Slovakia. *Atmosphere*, *11*(8), 821. https://doi.org/10.3390/atmos11080821

Skamarock, W. C., Klemp, J. B., Dudhia, J., Gill, D. O., Liu, Z., Berner, J., et al. (2019). *A description of the advanced research WRF model version 4* (p. 162). NCAR Technical Note NCAR/TN-556+STR. National Center for Atmospheric Research: Boulder, CO, USA.

Sobash, R. A., Kain, J. S., Bright, D. R., Dean, A. R., Coniglio, M. C., & Weiss, S. J. (2011). Probabilistic forecast guidance for severe thunderstorms based on the identification of extreme phenomena in convection allowing model forecasts. *Weather and Forecasting*, *26*(5), 714–728. https://doi.org/10.1175/WAF-D-10-05046.1

Sobash, R. A., Romine, G. S., Schwartz, C. S., Gagne, D. J., & Weisman, M. L. (2016). Explicit forecasts of low-level rotation from convection-allowing models for next-day tornado prediction. *Weather and Forecasting*, *31*(5), 1591–1614. https://doi.org/10.1175/WAF-D-16-0073.1

Sobash, R. A., Schwartz, C. S., Romine, G. S., & Weisman, M. L. (2019). Next-day prediction of tornadoes using convection-allowing models with 1-km horizontal grid spacing. *Weather and Forecasting*, *34*(4), 1117–1135. https://doi.org/10.1175/WAF-D-19-0044.1

Taszarek, M., Allen, J. T., Groenemeijer, P., Edwards, R., Brooks, H. E., Chmielewski, V., & Enno, S. E. (2020). Severe convective storms across Europe and the United States. Part I: Climatology of lightning, large hail, severe wind, and tornadoes. *Journal of Climate*, *33*(23), 10239–10261. https://doi.org/10.1175/JCLI-D-20-0345.1

Taszarek, M., Allen, J. T., Púčik, T., Hoogewind, K. A., & Brooks, H. E. (2020). Severe convective storms across Europe and the United States. Part II: ERA5 environments associated with lightning, large hail, severe wind, and tornadoes. *Journal of Climate*, *33*(23), 10263–10286. https://doi.org/10.1175/JCLI-D-20-0346.1

Taszarek, M., & Gromadzki, J. (2017). Deadly tornadoes in Poland from 1820 to 2015. *Monthly Weather Review*, *145*(4), 1221–1243. https://doi.org/10.1175/MWR-D-16-0146.1

Taszarek, M., Pilguj, N., Allen, J. T., Gensini, V. A., Brooks, H. E., & Szuster, P. (2021). Comparison of convective parameters derived from ERA5 and MERRA2 with sounding data over Europe and North America. *Journal of Climate*, *34*(8), 3211–3255. https://doi.org/10.1175/JCLI-D-20-0484.1

Thompson, G., Field, P. R., Rasmussen, R. M., & Hall, W. D. (2008). Explicit forecasts of winter precipitation using an improved bulk microphysics scheme. Part II: Implementation of a new snow parameterization. *Monthly Weather Review*, *136*(12), 5095–5115. https://doi.org/10.1175/2008MWR2387.1

Thompson, R. L., Edwards, R., Hart, J. A., Elmore, K. L., & Markowski, P. (2003). Close proximity soundings within supercell environments obtained from the rapid update cycle. *Weather and Forecasting*, *18*(6), 1243–1261. https://doi.org/10.1175/1520-0434(2003)018<1243:cpswse>2.0.co;2

Thompson, R. L., Smith, B. T., Dean, A., & Marsh, P. (2013). Spatial distributions of tornadic near-storm environments by convective mode. *The Electronic Journal of Severe Storms Meteorology*, *8*(5). Retrieved from http://www.ejssm.org/ojs/index.php/ejssm/article/viewArticle/125

Thompson, R. L., Smith, B. T., Grams, J. S., Dean, A. R., & Broyles, C. (2012). Convective modes for significant severe thunderstorms in the contiguous United States. Part II: Supercell and QLCS tornado environments. *Weather and Forecasting*, *27*(5), 1136–1154. https://doi.org/10.1175/WAF-D-11-00116.1

Tochimoto, E., & Niino, H. (2016). Structural and environmental characteristics of extratropical cyclones that cause tornado outbreaks in the warm sector: A composite study. *Monthly Weather Review*, *144*(3), 945–969. https://doi.org/10.1175/MWR-D-15-0015.1

Tochimoto, E., & Niino, H. (2017). Structural and environmental characteristics of extratropical cyclones associated with tornado outbreaks in the warm sector: An idealized numerical study. *Monthly Weather Review*, *145*(1), 117–136. https://doi.org/10.1175/MWR-D-16-0107.1

Trapp, R. J., Robinson, E. D., Baldwin, M. E., Diffenbaugh, N. S., & Schwedler, B. R. (2011). Regional climate of hazardous convective weather through high-resolution dynamical downscaling. *Climate Dynamics*, *37*(3), 677–688. https://doi.org/10.1007/s00382-010-0826-y

Trier, S. B., Romine, G. S., Ahijevych, D. A., Sobash, R. A., & Chasteen, M. B. (2021). Relationship of convection initiation and subsequent storm strength to ensemble simulated environmental conditions during IOP3b of VORTEX Southeast 2017. *Monthly Weather Review*, *149*(10), 3265–3287. https://doi.org/10.1175/MWR-D-21-0111.1

van Delden, A. (2001). The synoptic setting of thunderstorms in Western Europe. *Atmospheric Research*, *56*(1–4), 89–110. https://doi.org/10.1016/S0169-8095(00)00092-2

van den Broeke, M. S., Schultz, D. M., Johns, R. H., Evans, J. S., & Hales, J. E. (2005). Cloud-to-ground lightning production in strongly forced, low-instability convective lines associated with damaging wind. *Weather and Forecasting*, *20*(4), 517–530. https://doi.org/10.1175/WAF876.1

Varga, Á. J., & Breuer, H. (2021). Evaluation of convective parameters derived from pressure level and native ERA5 data and different resolution WRF climate simulations over Central Europe. *Climate Dynamics*, *58*, 1569–1585. https://doi.org/10.1007/s00382-021-05979-3

Wade, A. R., & Parker, M. D. (2021). Dynamics of simulated high-shear, low-CAPE supercells. *Journal of the Atmospheric Sciences*, *78*(5), 1389–1410. https://doi.org/10.1175/JAS-D-20-0117.1

Wesolek, E., & Mahieu, P. (2011). The F4 tornado of August 3, 2008, in Northern France: Case study of a tornadic storm in a low CAPE environment. *Atmospheric Research*, *100*(4), 649–656. https://doi.org/10.1016/j.atmosres.2010.09.003

Zanini, M. A., Hofer, L., Faleschini, F., & Pellegrino, C. (2017). Building damage assessment after the Riviera del Brenta tornado, northeast Italy. *Natural Hazards*, *86*, 1247–1273. https://doi.org/10.1007/s11069-017-2741-6

Zheng, Y., Alapaty, K., Herwehe, J. A., Del Genio, A. D., & Niyogi, D. (2016). Improving high-resolution weather forecasts using the Weather Research and Forecasting (WRF) Model with an updated Kain-Fritsch scheme. *Monthly Weather Review*, *144*(3), 833–860. https://doi.org/10.1175/MWR-D-15-0005.1